Proceedings of the XVI National Conference on Superconductivity and Strongly Correlated Systems, Zakopane 2013

t–t'–J–U Model in Mean-Field Approximation: Coexistence of Superconductivity and Antiferromagnetism

M. Abram*

Marian Smoluchowski Institute of Physics, Jagiellonian University, W.S. Reymonta 4, 30-059 Kraków, Poland

We discuss the t–J–U model in the mean-field approximation. The role of spin-exchange coupling J and the second nearest hopping t' are examined in the context of the coexistence of superconductivity and antiferromagnetism. Stability of the phases is studied with respect to temperature. The coexistence region exists for the sufficiently large Coulomb repulsion ($U > U_{\mathrm{cr}}$), and in the vicinity of the half-filled band (hole doping $\delta < \delta_{\mathrm{cr}}$). The critical hole doping is relatively small ($\delta_{\mathrm{cr}} \approx 0.006$ for $J/|t| = 1/3$) and linear with respect to J. The decrease of U_{cr} is proportional to J, except the limit of small J ($J/|t| < 0.03$), where U_{cr} grows rapidly with decreasing J. The effect of the second nearest hopping is limited — the phase diagram does not change in a qualitative manner when the t' value is changed. In the limit of $T \to 0$, SC phase is stable even for large hole-doping (such as $\delta = 0.5$). Additional paramagnetic phase appears for large δ or small U at non-zero temperature. When temperature increases, both SC and AF+SC phase regions are reduced.

DOI: 10.12693/APhysPolA.126.A-25

PACS: 71.27.+a, 74.25.Dw, 74.72.Gh

1. Introduction

One of the basic models for high-temperature superconductors and correlated systems is t–J model, which can be derived from the Hubbard model in the limit of large Coulomb repulsion U [1, 2]. In the simplest version the t–J model has the form [1–4]:

$$\hat{\mathcal{H}}_{t-J} = \sum_{i\neq j,\,\sigma} \hat{\mathcal{P}}_0\, t_{ij} \hat{c}^{\dagger}_{i\sigma} \hat{c}_{j\sigma}\, \hat{\mathcal{P}}_0 + \sum_{i\neq j} J_{ij}\, \hat{\mathcal{P}}_0 \left(\boldsymbol{S}_i \cdot \boldsymbol{S}_j - \frac{1}{4} \hat{n}_i \hat{n}_j \right) \hat{\mathcal{P}}_0, \tag{1}$$

where t_{ij} is the hopping integral, $J_{ij} \equiv 4t^2_{ij}/U$ is the kinetic-exchange integral, and $\hat{\mathcal{P}}_0 = \prod_i (1 - \hat{n}_{i\uparrow}\hat{n}_{i\downarrow})$ is the Gutzwiller projector operator eliminating the double site occupancies. Sometimes, for simplicity, the term $\frac{1}{4}\hat{n}_i\hat{n}_j$ is neglected (cf. discussion of the term's relevance in Ref. [5, Ch. 9]).

For the Hubbard model, the energy cost for two electrons residing on the same site is equal to U, hence in the limit of $U \to +\infty$ (which was assumed when deriving the t–J model [1]), the double occupancies are prohibited. It is realized through the projector $\hat{\mathcal{P}}_0$ which eliminates them. Alternatively, interaction term of the Hubbard type, $U \sum_i \hat{n}_{i\uparrow}\hat{n}_{i\downarrow}$, can be added to the Hamiltonian (1) explicitly. In such situation and for sufficiently large U, the energy of the double occupancies is high so that they effectively are not present in the system. In effect, the projector $\hat{\mathcal{P}}_0$ can be omitted (cf. e.g. Ref. [6], where such approach was formulated).

However, one could argue that e.g. for the cuprates, the term proportional to J_{ij} does not only reflect the kinetic exchange interactions of d-holes in the Cu plane, but also incorporates effects of the Cu–O hybridization, hence the $J_{ij} \equiv 4t^2_{ij}/U$ identity is no longer valid [7]. Furthermore, the Cu-O hybridization can reduce the cost of double occupancy, and the requirement of large U may no longer be necessary. Thus, the enlarged Hamiltonian becomes effective and all three parameters, t_{ij}, J_{ij}, and U, can now be treated as independent parameters. This can be regarded as rationale for introducing the t–J–U model.

The t–J–U model was extensively studied by Zhang [8], Gan et al. [9, 10], and Bernevig et al. [11]. However, no antiferromagnetic order was considered in those works†.

Recently, we have covered the topic (cf. Ref. [13]) and we have found that in the t–J–U model for sufficiently large U, a coexistence of antiferromagnetism and superconductivity (AF+SC) appears, but only in a very limited hole-doping (close range to the half-filled band). The present article is an extension of the previous work [13]. The model is refined to consider also the second nearest-neighbor hopping.

The structure of this paper is as follows: in Sect. 2 the model is defined, as well as the approximations leading to the effective single-particle Hamiltonian. In Sect. 3 the details of the solving procedure are provided. Results and discussions are presented in Sects. 4 and 5, respectively.

*e-mail: marcin.abram@uj.edu.pl

†Some attempts was made by some authors, cf. Ref. [12], but their method suffered of some inconsistencies (cf. discussion in Ref. [13]).

2. The model and the effective single-particle Hamiltonian

The starting Hamiltonian for t–J–U model has the form [8–10]:

$$\hat{\mathcal{H}}=\sum_{i\neq j,\,\sigma} t_{ij}\hat{c}^{\dagger}_{i\sigma}\hat{c}_{j\sigma}+\sum_{i\neq j} J_{ij}\,\boldsymbol{S}_i\cdot\boldsymbol{S}_j+U\sum_i \hat{n}_{i\uparrow}\hat{n}_{i\downarrow}, \quad (2)$$

where t_{ij} denotes the hopping term, J_{ij} the spin-exchange coupling, U the on-site Coulomb repulsion, $\hat{c}^{\dagger}_{i\sigma}$ ($\hat{c}_{i\sigma}$) are creation (annihilation) operators of an electron on site i and with spin σ; $\hat{n}_{i\sigma}\equiv\hat{c}^{\dagger}_{i\sigma}\hat{c}_{i\sigma}$ denotes electron number operator, $\boldsymbol{S}_i\equiv(\hat{S}^x_i,\,\hat{S}^y_i,\,\hat{S}^z_i)$ spin operator. In the fermion representation $\hat{S}^{\sigma}_i\equiv\frac{1}{2}(\hat{S}^x_i+\sigma\hat{S}^y_i)=\hat{c}^{\dagger}_{i\sigma}\hat{c}_{i\sigma}$, while $\hat{S}^z_i=\frac{1}{2}(\hat{n}_{i\uparrow}-\hat{n}_{i\downarrow})$.

Here, we consider a two-dimensional, square lattice. This is justified since cuprates have a quasi two--dimensional structure. We assume that $J_{ij}\equiv J/2$ if i, j indicate the nearest neighbors, and $J_{ij}=0$ otherwise. We restrict hopping to the first (t) and the second nearest neighbors (t'). We use the Gutzwiller approach (GA) [14, 15] to obtain an effective single-particle Hamiltonian. Specifically, to calculate the average $\langle\hat{\mathcal{H}}\rangle\equiv\langle\Psi\mid\hat{\mathcal{H}}\mid\Psi\rangle$, the form of $|\Psi\rangle$ has to be known. We are assuming that $|\Psi\rangle\approx|\Psi_G\rangle\equiv\hat{P}_G|\Psi_0\rangle=\prod_i\left(1-(1-g)\hat{n}_{i\uparrow}\hat{n}_{i\downarrow}\right)|\Psi_0\rangle$, where g is a variational parameter and $|\Psi_0\rangle$ is a single-particle wave function. Let us note that for $g=0$ the projector cuts off all states with double occupation (two electrons on one site), while for $g=1$ we have simple $|\Psi_G\rangle=|\Psi_0\rangle$. In GA, we assume that

$$\frac{\langle\Psi_G\mid\mathcal{H}\mid\Psi_G\rangle}{\langle\Psi_G\mid\Psi_G\rangle}=\langle\Psi_0\mid\hat{\mathcal{H}}_{\rm eff}\mid\Psi_0\rangle\equiv\langle\hat{\mathcal{H}}_{\rm eff}\rangle_0, \quad (3)$$

where

$$\begin{aligned}\hat{\mathcal{H}}_{\rm eff}&=t\sum_{\langle i,j\rangle,\sigma} g_{i\sigma}g_{j\sigma}\left(\hat{c}^{\dagger}_{i\sigma}\hat{c}_{j\sigma}+\mathrm{H.c.}\right)\\&+t'\sum_{\langle\langle i,j\rangle\rangle,\sigma} g_{i\sigma}g_{j\sigma}\left(\hat{c}^{\dagger}_{i\sigma}\hat{c}_{j\sigma}+\mathrm{H.c.}\right)\\&+J\sum_{\langle i,\,j\rangle,\,\sigma} g^s_i g^s_j\,\boldsymbol{S}_i\cdot\boldsymbol{S}_j+U\sum_i\hat{n}_{i\uparrow}\hat{n}_{i\downarrow},\end{aligned} \quad (4)$$

where $\sum_{\langle i,j\rangle}$ and $\sum_{\langle\langle i,j\rangle\rangle}$ denotes summation over all unique pairs of first and second nearest neighbors, H.c. is the Hermitian conjugation, and $g_{i\sigma}$, g^s_i are renormalization factors [16, 17]

$$g_{i\sigma}=\sqrt{g^s_i}\left(\sqrt{\frac{(1-n_{i\bar{\sigma}})(1-n+d^2)}{1-n_{i\sigma}}}+\sqrt{\frac{n_{i\bar{\sigma}}\,d^2}{n_{i\sigma}}}\right), \quad (5)$$

$$g^s_i=\frac{n-2d^2}{n-2n_{i\sigma}n_{i\bar{\sigma}}}, \quad (6)$$

with $n\equiv\langle\hat{n}_{i\uparrow}+\hat{n}_{i\downarrow}\rangle_0$, $d^2\equiv\langle\hat{n}_{i\uparrow}\hat{n}_{i\downarrow}\rangle_0$, and

$$n_{i\sigma}\equiv\langle\hat{c}^{\dagger}_{i\sigma}\hat{c}_{i\sigma}\rangle_0\equiv\frac{1}{2}\left(n+\sigma\,\mathrm{e}^{\mathrm{i}\boldsymbol{Q}\cdot\boldsymbol{R}_i}\,m\right), \quad (7)$$

where m is (bare) sublattice magnetization per site, $\boldsymbol{Q}\equiv(\pi,\,\pi)$, and $\boldsymbol{R}_i$ is the position vector of site i. We divide the lattice into two sublattices, A where on average the spin is *up*, and B where on average is *down* (cf. Fig. 1). Thus $n_{i\in A,\sigma}\equiv\frac{1}{2}\left(n+\sigma m\right)$, and $n_{i\in B,\sigma}\equiv\frac{1}{2}\left(n-\sigma m\right)$.

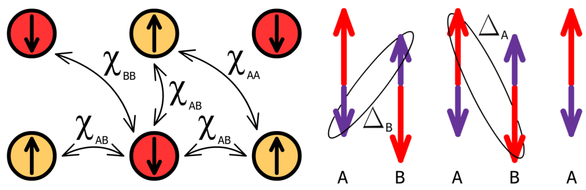

Fig. 1. Schematic interpretation of χ, $\chi_{\rm AA}$ and $\chi_{\rm BB}$ (left part) and $\Delta_{\rm A}$ and $\Delta_{\rm B}$ (right part). To consider antiferromagnetism in the system, we can divide the lattice into two sublattices, A where in average the spin is *up*, and B where in average is *down*. Thus χ denotes hopping between sites belonging to sublattices A and B, while $\chi_{\rm AA}$ and $\chi_{\rm BB}$ hopping within one sublattice (A or B, respectively); $\Delta_{\rm A}$ denotes pairing of majority spins (*up* from sublattice A and *down* from B), and $\Delta_{\rm B}$ pairing of minority spins (*up* from B and *down* from A).

We define average hopping amplitude for the first and the second nearest neighbors (n.n.) as:

$$\chi_{ij\sigma}\equiv\langle\hat{c}^{\dagger}_{i\sigma}\hat{c}_{j\sigma}\rangle_0\equiv\begin{cases}\chi & \text{for 1st nearest neighbor,}\\ \chi_S+\sigma\,\mathrm{e}^{\mathrm{i}\boldsymbol{Q}\cdot\boldsymbol{R}_i}\chi_T & \text{for 2nd nearest neighbor,}\end{cases} \quad (8)$$

where $\chi\equiv\chi_{\rm AB}$ denotes hopping between sublattices A and B (or vice versa, cf. left part in Fig. 1); $\chi_S\equiv\frac{1}{2}(\chi_{\rm AA}+\chi_{\rm BB})$ and $\chi_T\equiv\frac{1}{2}(\chi_{\rm AA}-\chi_{\rm BB})$, where $\chi_{\rm AA}$ and $\chi_{\rm BB}$ denotes hopping within one sublattice. We define also the electron pairing between nearest neighbors as

$$\Delta_{ij\sigma}\equiv\langle\hat{c}_{i\sigma}\hat{c}_{j\bar{\sigma}}\rangle_0=-\tau_{ij}\left(\sigma\Delta_S+\mathrm{e}^{\mathrm{i}\boldsymbol{Q}\cdot\boldsymbol{R}_i}\Delta_T\right), \quad (9)$$

where $\tau_{ij}\equiv1$ for $j=i\pm\hat{x}$, and $\tau_{ij}\equiv-1$ for $j=i\pm\hat{y}$ to ensure d-wave symmetry. $\Delta_S\equiv\frac{1}{4}\left(\Delta_{\rm A}+\Delta_{\rm B}+\mathrm{H.c.}\right)$ and $\Delta_T\equiv\frac{1}{4}\left(\Delta_{\rm A}-\Delta_{\rm B}+\mathrm{H.c.}\right)$, cf. right part in Fig. 1. We assume that all the above averages: χ, χ_S, χ_T, Δ_S, and Δ_T, are real. Finally, we are able to calculate the average $W\equiv\langle\hat{\mathcal{H}}\rangle_0$, which has the form

$$\begin{aligned}\frac{W}{\Lambda}&=8g_t t\chi+4g^{\max}_{t'}t'\chi_S+4g^{\min}_{t'}t'\chi_S)\\&+g_sJ\left(-\frac{1}{2}m^2-3\chi^2-3\Delta_S^2+\Delta_T^2\right)+Ud^2,\end{aligned} \quad (10)$$

where the renormalization factors $g_t\equiv g_{i\in{\rm A}\sigma}g_{j\in{\rm B}\sigma}$, $g^{\max}_{t'}\equiv g_{i\in{\rm A}\uparrow}g_{j\in{\rm A}\uparrow}$, $g^{\min}_{t'}\equiv g_{i\in{\rm A}\downarrow}g_{j\in{\rm A}\downarrow}$, and $g_s\equiv g^s_{i\in{\rm A}}g^s_{j\in{\rm B}}$.

3. Statistically-consistent Gutzwiller approximation

To determine the stable phases and their characteristics (sublattice magnetization, SC gap, etc.) we construct the grand potential functional, which we next minimize with respect to all parameters. However, to ensure that the averages calculated in a self-consistent manner are equal to those obtained variationally, we first use the so-called statistically-consistent Gutzwiller approximation (SGA) (cf. introduction to SGA [18], and examples of its use in the context of the t–J model [19, 20], the t–J–U model [13], the Anderson–Kondo lattice model [21, 22], the extended Hubbard models [23–25], or the liquid ^{3}He [26]). Here, we impose constraints on each average, which is present in Eq. (10). Hence, our effective Hamiltonian takes the form

$$\hat{K} = W - \sum_{\langle i,j\rangle,\sigma} \left(\lambda^{\chi}_{ij\sigma}\left(\hat{c}^{\dagger}_{i\sigma}\hat{c}_{j\sigma} - \chi_{ij\sigma}\right) + \text{H.c.}\right)$$
$$- \sum_{\langle\langle i,j\rangle\rangle,\sigma} \left(\lambda^{\chi}_{ij\sigma}\left(\hat{c}^{\dagger}_{i\sigma}\hat{c}_{j\sigma} - \chi_{ij\sigma}\right) + \text{H.c.}\right)$$
$$- \sum_{\langle i,j\rangle} \left(\lambda^{\Delta}_{ij\sigma}\left(\hat{c}_{i\sigma}\hat{c}_{j\bar{\sigma}} - \Delta_{ij\sigma}\right) + \text{H.c.}\right)$$
$$- \sum_{i\sigma} \left(\lambda^{n}_{i\sigma}\left(\hat{n}_{i\sigma} - n_{i\sigma}\right)\right) - \mu \sum_{i\sigma} \hat{n}_{i\sigma}, \tag{11}$$

where we have also introduced the chemical potential term $-\mu\sum_{i\sigma}\hat{n}_{i\sigma}$. Symbols $\{\lambda_i\}$ stand for Lagrange multipliers, having the same form as the corresponding to them averages, namely

$$\lambda^{n}_{i\sigma} = \frac{1}{2}\left(\lambda_n + \sigma\,\mathrm{e}^{\mathrm{i}\boldsymbol{Q}\cdot\boldsymbol{R}_i}\lambda_m\right), \tag{12a}$$

$$\lambda^{\chi}_{ij\sigma} \equiv \begin{cases} \lambda_{\chi} & \text{for 1st n.n.,} \\ \lambda_{\chi_S} + \sigma\,\mathrm{e}^{\mathrm{i}\boldsymbol{Q}\cdot\boldsymbol{R}_i}\lambda_{\chi_T} & \text{for 2nd n.n.,} \end{cases} \tag{12b}$$

$$\lambda^{\Delta}_{ij\sigma} = -\tau_{ij}\left(\sigma\lambda_{\Delta_S} + \mathrm{i}\,\mathrm{e}^{\mathrm{i}\boldsymbol{Q}\cdot\boldsymbol{R}_i}\lambda_{\Delta_T}\right). \tag{12c}$$

In the next step we diagonalize the grand Hamiltonian $\hat{K}$ and construct the grand potential functional $\mathcal{F} = -\frac{1}{\beta}\ln\mathcal{Z}$, where $\beta = 1/k_{\mathrm{B}}T$, and $\mathcal{Z} = \mathrm{Tr}\left(\mathrm{e}^{-\beta\hat{K}}\right)$. The minimization conditions for determining all quantities and Lagrange multiplies are

$$\frac{\partial\mathcal{F}}{\partial A_i} = 0, \quad \frac{\partial\mathcal{F}}{\partial\lambda_i} = 0, \quad \frac{\partial\mathcal{F}}{\partial d} = 0, \tag{13}$$

where $\{A_i\}$ denote here all 7 averages: χ, χ_S, χ_T, Δ_S, Δ_T, n, and m, while $\{\lambda_i\}$ denote all Lagrange multipliers λ_χ, λ_{χ_S}, λ_{χ_T}, λ_{Δ_S}, λ_{Δ_T}, λ_n, and λ_m. The system of equations is solved self-consistently. To determine the stability of physical phases, free energy has to be calculated according to the prescription

$$F = \mathcal{F}_0 + \Lambda\mu n, \tag{14}$$

where $\mathcal{F}_0$ is the value of the grand potential functional $\mathcal{F}$ at minimum, and Λ is the number of lattice sites.

4. Results

The numerical calculations were carried out using GNU Scientific Library (GSL) [27] for a two-dimensional, square lattice of $\Lambda = 512 \times 512$ size, and unless stated otherwise, $t = -1$, $J = |t|/3$, and $\beta|t| = 1500$ (it was checked that for such large $\beta \equiv 1/k_{\mathrm{B}}T$ we have effectively $T = 0$).

Here, χ, χ_S, χ_T, Δ_S, Δ_T, and m are bare averages. Renormalized by a proper Gutzwiller factors, they become order parameters of the corresponding phases. Thus: $\chi^c \equiv g_t\chi$, $\chi^c_S \equiv g_{t'}\chi_S$, $\chi^c_T \equiv g_{t'}\chi_T$, $\Delta^c_S \equiv g_\Delta\Delta_S$, $\Delta^c_T \equiv g_\Delta\Delta_T$, and $m^c = g_m m$, where (cf. Eqs. (5) and (6)), $g_t \equiv g_{i\in\mathrm{A}\sigma}g_{j\in\mathrm{B}\sigma}$, $g_{t'} \equiv \frac{1}{2}(g_{i\in\mathrm{A}\uparrow}g_{j\in\mathrm{A}\uparrow} + g_{i\in\mathrm{A}\downarrow}g_{j\in\mathrm{A}\downarrow})$, $g_\Delta \equiv \frac{1}{2}\left(g_{i\in\mathrm{A}\uparrow}g_{i\in\mathrm{B}\downarrow} + g_{i\in\mathrm{A}\downarrow}g_{i\in\mathrm{B}\uparrow}\right)$, and $g_m \equiv g^s_{i\in\mathrm{A}}g^s_{j\in\mathrm{B}}$.

4.1. Results for t–J–U model, for $t' = 0$

In the limit of the low temperature ($T \to 0$, i.e. $\beta \to +\infty$) the SC phase is stable for any value of $\delta > 0$, $U > 0$, or $J > 0$. For sufficiently large Coulomb repulsion ($U > U_{\mathrm{cr}}$) and for small hole doping ($\delta < \delta_{\mathrm{cr}}$), a coexistent AF+SC phase can be found (cf. Fig. 2). For $\delta = 0$ and for $U > U_{\mathrm{cr}}$ we obtain the Mott insulating state. For $\delta = 0$ and $U < U_{\mathrm{cr}}$ electrons can have double occupancies ($d^2 \neq 0$) and the superconducting pairing is maintained (such a feature in literature is called the gossamer superconductivity [28]).

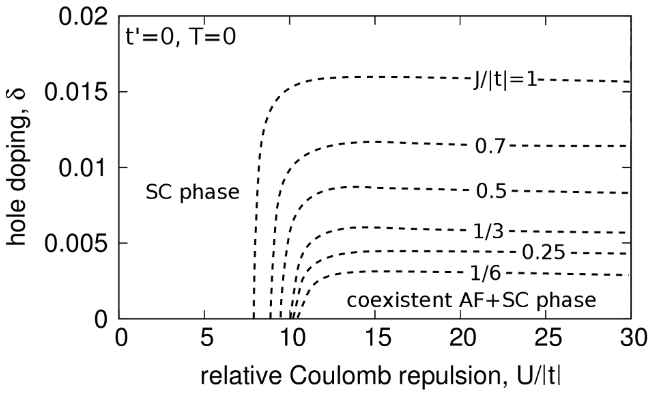

Fig. 2. The AF+SC coexistence region for $t' = 0$, $T = 0$, and different values of the the exchange coupling J (in units of t).

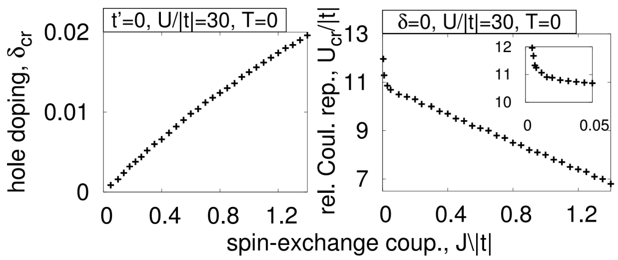

Fig. 3. In the left part, the effect of the spin-exchange coupling J on the critical hole doping (δ_{cr}). In the right part, the effect of J on the critical relative Coulomb repulsion (U_{cr}). Let us note that $\delta_{\mathrm{cr}}(J)$ is quasi-linear in the whole range of the tested parameter, while for $U_{\mathrm{cr}}(J)$ we observe non-linear behavior for $J/|t| < 0.03$ (cf. the inset in the right part).

The influence of the spin-exchange coupling J on the range of the coexistence region AF+SC was examined. δ_{cr} is a linear function of J (cf. the left part in Fig. 3), while the critical Coulomb repulsion U_{cr} has non-linear behavior for $J/|t| < 0.03$ (the value of U_{cr} grows rapidly when J decrease, cf. the right part in Fig. 3).

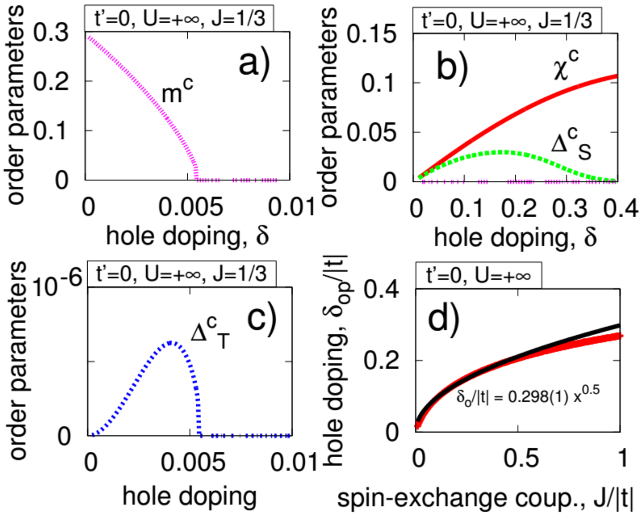

Fig. 4. In the parts (a)–(c), selected order parameters as a function of doping δ are presented. Let us note that $\Delta_T \neq 0$ only if $m^c \neq 0$. In the part (d), the optimal doping for a singled SC gap (Δ^c_S) is shown, as a function of the exchange coupling J, in $U \to +\infty$ limit (red line). The black line is a numerical fit, $f(x) = 0.298(1)\, x^{0.5}$.

For $U \to +\infty$ we reproduce the results of the t–J model. As was checked, even for not too large U the convergence to t–J model results is sufficient. For instance, for $U = 30$ our results match those for the t–J model (so the limit $U = +\infty$) within less than 1% error, and for $U = 100$ within an error of less than 0.1%. In Fig. 4 in parts (a)–(c), the correlated states χ^c, Δ^c_S, Δ^c_T, m^c, and d^2 are presented for $U = 100$ and $\beta|t| = 1500$ (effectively $U = +\infty$ and $T = 0$). Let us note that the staggered component of the superconducting gap (Δ_T) is very small and appears only when $m^c \neq 0$, i.e., in the AF+SC phase. However, Δ_T value is very small when compared to value of Δ_S (there is $\Delta^c_T/\Delta^c_S < 10^{-4}$), thus its effect can be practically neglected[‡].

In the last part (d) in Fig. 4 we show (red line) the optimal doping δ_{op} for singled SC gap (Δ^c_S) as a function of J. The black line in this part is a function $f \sim \sqrt{J/|t|}$, numerically fitted to the data.

4.2. A significance of the second nearest neighbors hopping t'

The influence of the second nearest neighbors hopping term t' is exhibited in Fig. 5. Let us note that the critical Coulomb repulsion for AF+SC phase (U_{cr}) is practically independent of the value of t' (it was checked, $U_{\mathrm{cr}}(t' = 0)$ and $U_{\mathrm{cr}}(t' = 1)$ differ about 1%). The critical doping (δ_{cr}) is more susceptible to the value of t', but note that the typical value of the t' ranges from $-0.1t$ to $-0.5t$ (cf. Ref. [29, Ch. 7.1.2]), and in such a range δ_{cr} changes only about 10%.

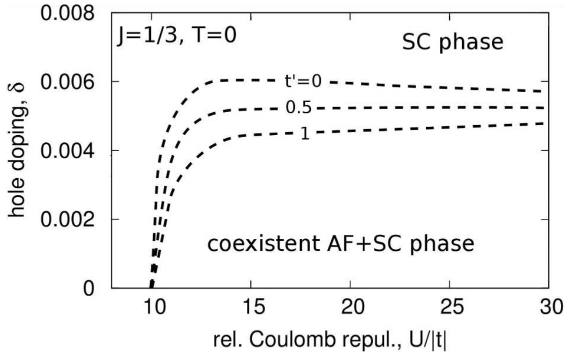

Fig. 5. Significance of the second nearest neighbors hopping. Values of t' are given in units of t. The presence of t' does not change the AF+SC range in qualitative manner.

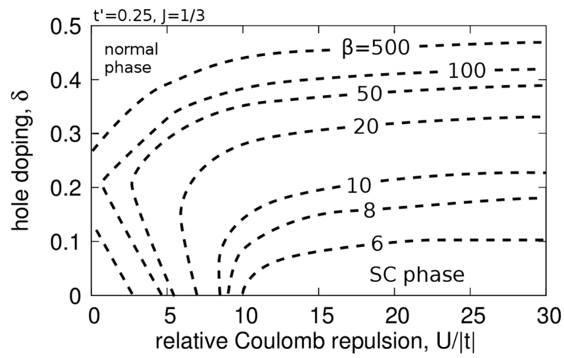

Fig. 6. The effect of the temperature (meassured in units of $|t|$) on the stability of SC phase in t–t'–J–U model ($t = -1$, $t' = 0.25$). The dashed lines correspond to the range of SC phase for $\beta = 500$ ($T \sim 5$–12 K), $\beta = 100$ (25–60 K), $\beta = 50$ (50–120 K), $\beta = 20$ (130–290 K), $\beta = 10$ (250–580 K), $\beta = 8$ (320–720 K), $\beta = 6$ (420–1000 K).

4.3. Nonzero temperature

In the limit of the zero temperature, for small U or/and large δ, the value of the SC order parameter Δ^c_S is small, but still nonzero. Increasing the temperature (decreasing the parameter β), the paramagnetic (PM) phase appears in region where the order parameter of SC phase was weak (cf. Fig. 6). For large T (small β), the range of the SC phase is reduced to the vicinity of the Mott-insulator phase ($\delta \gtrsim 0$, and $U > U_{\mathrm{cr}}$).

The measured value of the hopping term t for the cuprates ranges from 0.22 eV to 0.5 eV (cf. Ref. [30, Ch. 7.1.2]). Hence the $\beta|t| = 1500$ corresponds to the temperature 2–4 K, $\beta|t| = 500$ to 5–12 K, $\beta|t| = 100$ to 25–60 K, $\beta|t| = 50$ to 50–120 K, $\beta|t| = 20$ to 130–290 K, $\beta|t| = 10$ to 250–580 K, $\beta|t| = 8$ to 320–720 K, $\beta|t| = 6$ to 420–1000 K.

[‡]The free energy F_0 in minimum (for $T = 0$) is equal to W (cf. Eq. (10)). If $\Delta^c_T/\Delta^c_S \equiv \Delta_T/\Delta_S < 10^{-4}$ then the impact of Δ^c_T for the final energy of the solution is about 10^{-8} smaller than the impact of Δ^c_S. Thus Δ_T in practical calculations can be neglected.

5. Conclusions

In this work, the t–t'–J–U model was studied in the SGA scheme which plays the role of the mean-field approximation. In the limit of the zero temperature, three phases were found: superconductivity (SC), coexistent antiferromagnetic-superconducting state (AF+SC), and the Mott-insulating phase (for the half filling). The AF+SC phase exists only for sufficiently large Coulomb repulsion ($U > U_{\rm cr}$) and for small hole doping ($\delta < \delta_{\rm cr}$). We have shown how the range of AF+SC coexistence varies with J and t'. The impact of J was significant, both for $U_{\rm cr}$ and for $\delta_{\rm cr}$. However, the impact of t' was much smaller and in the range of physical values (for cuprates $t' \sim 0.1$–$0.5|t|$), it can be marginal.

The impact of the non-zero temperatures was tested. For $T > 0$, additionally to SC and AF+SC phases, a paramagnetic phase (normal phase) appears. The ranges of SC and AF+SC phases decrease with the temperature, but they remain stable even for relatively high temperature (≈ 1000 K). Such results, contradictory to the experiments, can be explained by the used method (the saddle-point method) and approximations used (the mean-field and the Gutzwiller approximation). To study more accurately the stability of the phases, more sophisticated method should be used (cf. e.g. the diagrammatic expansion for Gutzwiller-wave functions (DE-GWF) [29]).

Acknowledgments

I would like to express my gratitude to Prof. J. Spałek for his support and helpful detailed comments. I would also like to thank M. Wysokiński for discussions, and A. Hartnett for her critical reading of the manuscript. This research was supported by the Foundation for Polish Science (FNP) under the grant TEAM. Parts of the calculations were performed on the TERAACMIN supercomputer in the Academic Centre for Materials and Nanotechnology (ACMIN) of AGH University of Science and Technology in Kraków.

References

[1] J. Spałek, A.M. Oleś, *Physica B+C* **86-88**, 375 (1977); K.A. Chao, J. Spałek, A.M. Oleś, *J. Phys. C* **10**, L271 (1977).

[2] J. Spałek, *Acta Phys. Pol. A* **111**, 409 (2007).

[3] E. Dagotto, *Rev. Mod. Phys.* **66**, 763 (1994).

[4] P.A. Lee, N. Nagaosa, X.-G. Wen, *Rev. Mod. Phys.* **78**, 17 (2006).

[5] J. Jędrak, Ph.D. thesis, Jagiellonian University, Kraków 2011.

[6] H.Q. Lin, *Phys. Rev. B* **44**, 4674 (1991).

[7] F.C. Zhang, T.M. Rice, *Phys. Rev. B* **37**, 3759 (1988).

[8] F.C. Zhang, *Phys. Rev. Lett.* **90**, 207002 (2003).

[9] J.Y. Gan, F.C. Zhang, Z.B. Su, *Phys. Rev. B* **71**, 014508 (2005).

[10] J.Y. Gan, Y. Chen, Z.B. Su, F.C. Zhang, *Phys. Rev. Lett.* **94**, 067005 (2005).

[11] B.A. Bernevig, R.B. Laughlin, D.I. Santiago, *Phys. Rev. Lett.* **91**, 147003 (2003).

[12] F. Yuan, Q. Yuan, C.S. Ting, *Phys. Rev. B* **71**, 104505 (2005); H. Heiselberg, *Phys. Rev. A* **79**, 063611 (2009); K.-K. Voo, *J. Phys., Condens. Matter* **23**, 495602 (2011).

[13] M. Abram, J. Kaczmarczyk, J. Jędrak, J. Spałek, *Phys. Rev. B* **88**, 094502 (2013).

[14] M.C. Gutzwiller, *Phys. Rev. Lett.* **10**, 159 (1963).

[15] M.C. Gutzwiller, *Phys. Rev.* **137**, A1726 (1965).

[16] T. Ogawa, K. Kanda, T. Matsubara, *Prog. Theor. Phys.* **53**, 614 (1975).

[17] F.C. Zhang, C. Gros, T.M. Rice, H. Shiba, *Supercond. Sci. Technol.* **1**, 36 (1988).

[18] J. Jędrak, J. Kaczmarczyk, J. Spałek, arXiv:1008.0021, 2010, unpublished.

[19] J. Jędrak, J. Spałek, *Phys. Rev. B* **81**, 073108 (2010); J. Jędrak, J. Spałek, *Phys. Rev. B* **83**, 104512 (2011).

[20] J. Kaczmarczyk, J. Spałek, *Phys. Rev. B* **84**, 125140 (2011).

[21] O. Howczak, J. Spałek, *J. Phys., Condens. Matter* **24**, 205602 (2012).

[22] O. Howczak, J. Kaczmarczyk, J. Spałek, *Phys. Status Solidi B* **250**, 609 (2013).

[23] M. Zegrodnik, J. Spałek, J. Bünemann, *New J. Phys.* **15**, 073050 (2013).

[24] J. Spałek, M. Zegrodnik, *J. Phys. Condens. Matter* **25**, 435601 (2013).

[25] A.P. Kądzielawa, J. Spałek, J. Kurzyk, W. Wójcik, *Eur. Phys. J. B* **86**, 252 (2013).

[26] M.M. Wysokiński, J. Spałek, *J. Phys. Condens. Matter* **26**, 055601 (2014).

[27] M. Galassi, J. Davies, J. Theiler, B. Gough, P. Jungman, G. abd Alken, M. Booth, F. Rossi, *GNU Scientific Library Reference Manual*, 3rd ed., Network Theory, Ltd., London 2009.

[28] R.B. Laughlin, *Philos. Mag.* **86**, 1165 (2006).

[29] J. Kaczmarczyk, J. Spałek, T. Schickling, J. Bünemann, *Phys. Rev. B* **88**, 115127 (2013).

[30] N. Plakida, *High-Temperature Cuprate Superconductors: Experiment, Theory and Applications*, Springer, New York 2010.